

Received October 27, 2020, accepted November 21, 2020, date of publication December 1, 2020, date of current version January 13, 2021.

Digital Object Identifier 10.1109/ACCESS.2020.3041555

Investigation on Formation Mechanisms of Methanol During Cellulose Insulation Aging Based on Molecular Dynamics Simulation

JIEFENG LIU¹, (Member, IEEE), HUAN ZHAO¹, XIANHAO FAN¹, (Student Member, IEEE), AND YIYI ZHANG¹, (Member, IEEE)

Guangxi Key Laboratory of Power System Optimization and Energy Technology, Guangxi University, Nanning 530004, China

Corresponding author: Yiyi Zhang (yiyizhang@gxu.edu.cn)

This work was supported in part by the National Natural Science Foundation of China under Grant 61473272 and Grant 51867003, in part by the Natural Science Foundation of Guangxi under Grant 2018JJB160064 and Grant 2018JJA160176, in part by the Guangxi Bagui Young Scholars Special Funding, in part by the Boshike Award Scheme for Young Innovative Talents, in part by the Guangxi Key Laboratory of Power System Optimization and Energy Technology Project under Grant AE3020001829, and in part by the Basic Ability Improvement Project for Young and Middle-Aged Teachers in Universities of Guangxi under Grant 20190067 and Grant 20190046.

ABSTRACT In recent years, methanol has been proposed as a chemical indicator to assess the aging condition of cellulose insulation in oil-immersed power transformers. However, the formation mechanisms of methanol during cellulose degradation are not clear enough. In this paper, such formation mechanisms were studied using molecular dynamics simulation. Three main formation pathways of methanol were found and discussed. Analysis of the Mayer bonds of cellulose revealed that each atom of cellulose contributes differently to methanol formation. The methylol groups on the 5-carbon atom of the 1-pyran ring and 4-pyran ring of cellulose are more readily detached to form methanol molecules. In addition, changes in the amount of methanol molecule with simulation time were investigated. The results indicated that the separate existence of initial moisture and oxygen has no significant effect on the formation of methanol, while the co-existence of initial moisture and initial oxygen catalyzes the conversion of cellulose degradation products to methanol. The findings reported in this paper can provide a valuable theoretical basis for further studies on methanol as an indicator to evaluate the residual life of cellulose insulation.

INDEX TERMS Cellulose, methanol, molecular dynamics, cellulose insulation, formation mechanisms.

I. INTRODUCTION

The oil-immersed power transformer is an essential equipment of the power system for power conversion, distribution, and transmission [1]. It is generally accepted that the remaining life of the transformer is mainly determined by the aging condition of the cellulose insulation [2]–[8]. Currently, an authoritative criterion for assessing the aging condition of transformers is to measure the average viscometric degree of polymerization (DP_V) of the cellulose insulation. However, to obtain samples of cellulose insulation, the transformer needs to be de-energized, which inevitably causes economic losses of Electric Utilities. Determining the relationship between cellulose DP_V and specific products (chemical indicators) dissolved in the insulating oil is accepted by most researchers as an effective method to assess

the aging condition of cellulose insulation [9]. The carbon oxides (carbon monoxide and carbon dioxide), furanic compounds (2-furfuraldehyde), alcohols (methanol), etc. have been proposed as chemical indicators to evaluate the condition of cellulose insulation degradation [9], [10]. However, carbon oxides cannot accurately assess the aging condition of cellulose insulation since they could be also originated from oil decomposition in the long-term oxidation process. Besides, 2-furfuraldehyde (2-FAL) can hardly be detected in the thermally upgraded Kraft (TUK) paper, and it can be also produced by the degradation of hemicellulose [11]–[13]. Given the above drawbacks of the carbon oxides and furanic compounds, methanol has been proposed in recent years as a new chemical indicator to assess the aging condition of cellulose insulation [9], [13]. Some researches indicated that methanol could be a very promising chemical indicator to diagnose the degree of cellulose insulation degradation in power transformers [14], [15]. Jalbert *et al.* [9]

The associate editor coordinating the review of this manuscript and approving it for publication was Lin Lin¹.

proposed that there is a linear relationship between the number of ruptured 1,4- β -glycosidic bonds of cellulose and the amount of methanol, regardless of whether the cellulose insulation is ordinary or thermally-upgraded Kraft paper. The methanol content in some oil samples from the transformers of operating nuclear and coal-fired power plants in Belgium was analyzed [10]. It was found that no 2-furfuraldehyde (2-FAL), which has been used as a chemical indicator to diagnose the degree of cellulose insulation degradation since the mid-1980s, was detected, while some considerable amount of methanol was obtained in these oil samples. However, in these laboratory experiments, the chemical reaction mechanisms at atomic or molecular level are mainly investigated through analyzing the obtained experimental data, which is impossible to directly observe the moment of bonding and breaking [16]. Fortunately, the molecular dynamics simulation has developed rapidly, which makes the investigation on the chemical reaction mechanisms more accessible. The molecular structure, dynamics behavior, and physicochemical properties [16], [17] can be studied through the molecular dynamics simulation of individual molecules in the models of solids, liquids, and gases. Molecular dynamics can give a good approximation for physical movements of molecules and atoms, and it is an effective way to study the structure and function of biological macromolecules (e.g. proteins [18], [19] and cellulose [20], [21]). Molecular dynamics simulation focuses on the motion of molecules displaying the change of positions, velocities, and orientations [22]. During molecular dynamics simulation, a force field is needed in the system [23]. In general, the generic force field, such as DREIDING and UFF, cannot describe chemical reactivity, except for the Brenner potential. However, two important forces (i.e., the Coulomb interactions and van der Waals) are excluded in the Brenner potential. To solve this problem, Russo Jr and van Duin *et al.* [24], [25] proposed using the ReaxFF force field which includes the two forces to investigate the chemical reaction mechanisms. Chenoweth *et al.* [26] obtained the reaction rates of methane and benzene by applying the ReaxFF force field to molecular dynamics simulation of oxygenation of hydrocarbons. Ashraf *et al.* [27] adopted ReaxFF-MD to investigate the pyrolysis reaction mechanisms of binary fuel mixtures under supercritical conditions.

In this paper, the ReaxFF and ADF modules of Amsterdam Modeling Suite (AMS) simulation software were used to study the formation mechanisms of methanol during the degradation of cellulose insulation at the atomic or molecular level. The findings revealed that there are three main formation pathways of methanol during the degradation of cellulose insulation. In addition, the results indicated that the sources of carbon atoms and oxygen atoms constituting methanol mainly come from some specific atoms of cellobiose. Besides, it was found that the conversion of the degradation products of cellulose to methanol is catalyzed by the co-existence of initial moisture oxygen.

II. PRINCIPLE OF REAXFF FORCE FIELD

The ReaxFF is an empirical reactive force field that utilizes bond order (BO) to characterize the chemical interactions in a complex reaction system [24]–[29]. In this reaction system, the energy expression is shown in (1).

$$E_{\text{system}} = E_{\text{bond}} + E_{\text{val}} + E_{\text{pen}} + E_{\text{tors}} + E_{\text{conj}} + E_{\text{over}} + E_{\text{under}} + E_{\text{vdWaals}} + E_{\text{coulomb}} \quad (1)$$

where E_{bond} is the bonding energy, E_{val} is the valence-angle energy, E_{pen} is the penalty energy, E_{tors} is the torsion-angle energy, E_{conj} is the 4-body conjugation energy, E_{over} is the over-coordination energy, and E_{under} is the under-coordination energy. The noncovalent interactions comprise the van der Waals energy E_{vdWaals} and the Coulomb energy E_{coulomb} .

In the ReaxFF reaction system, the first step is to obtain the bond order between each atom pair after the position of each atom is recorded. Therefore, the calculation of bond order is the core of the ReaxFF force field, as shown in (2).

$$BO_{ij} = BO_{ij}^{\sigma} + BO_{ij}^{\pi} + BO_{ij}^{\pi\pi} = f(r_{ij}) \quad (2)$$

where r_{ij} is the distance between the i th and j th atoms. BO_{ij}^{σ} , BO_{ij}^{π} , and $BO_{ij}^{\pi\pi}$ are the bond order of single bond, double bond, and triple bond respectively. For the ReaxFF bond order, there are three main characteristics. First of all, the bond order has continuous dependence on the distance, which can be found from (2). Secondly, the transition of a total bond order from a nonbonded interaction to a bonded state is smooth [24]. Finally, the distance of bonding interactions in the ReaxFF is much farther than that in other reactive force fields.

III. CONSTRUCTION OF CELLULOSE MODEL

The DP_V of new Kraft paper insulation has the range of 1000–1200 [30], which is impractical to directly perform molecular dynamics simulation. Mazeau *et al.* [20] conducted molecular dynamics simulations with different cellulose DP_V. It was found that cellulose chains with different DP_V have the same molecular conformation and physical and chemical properties. Thus, the repeating unit of the cellulose chain (cellobiose molecule) was used as the simulation model with the consideration of computational power and efficiency [31], as shown in Fig. 1.

The temperature significantly influences the speed of the molecular transition. Sørensen and Voter *et al.* [32] proposed a temperature accelerated dynamics (TAD) method to extend the time scale of the simulation by orders of magnitude. The increase of temperature accelerates the chemical reactions, while the dynamics process at the original temperature remains unchanged. The original temperature refers to the temperature at which the corresponding molecular dynamics occurs without using the TAD method. During molecular dynamics simulation, if the temperature is higher, the reaction speed will be faster, and the simulation time will be shorter. In addition, it has been verified that the simulation

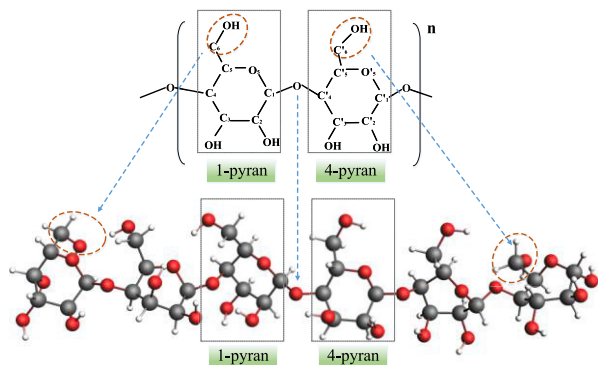


FIGURE 1. Chemical formula and molecular model of cellobiose. (Color code: carbon-gray, hydrogen-white, and oxygen-red).

results obtained by using the TAD are in good agreement with the experimental results [16], [27]. Considering that the simulation time was very long under ultra-low temperature and the formation pathway of methanol was difficult to track under ultra-high temperature, 3000 K was used to carry out molecular dynamics simulations in this paper.

The specific simulation steps were designed as follows:

First, 10 initial amorphous cellulose models with the same size ($30 \text{ \AA} \times 30 \text{ \AA} \times 30 \text{ \AA}$) were built by using the Builder module in the ReaxFF of AMS software. These initial cellulose models include 40 cellobiose molecules ($N = 1800$, which refers to the number of atoms), with an initial density of 0.85 g/cm^3 . To obtain the actual cellulose insulation density of 1.59 g/cm^3 [30], the NPT ensemble ($N = 1800$, $P = 1000 \text{ MPa}$, $T = 50 \text{ K}$) was used. During the density adjustment, high pressure ($P = 1000 \text{ MPa}$) was used to quickly adjust the initial density, and relatively low temperature ($T = 50 \text{ K}$) was set to prevent the system from chemical reactions. To verify the accuracy of the density adjustment, Fig. 2 shows changes in the density of the system and the number of cellobiose molecules in each reaction iteration step. It can be seen from Fig. 2 that the use of NPT ensemble during density adjustment can rapidly compress the density of cellulose model to actual cellulose density without causing cellulose degradation. After density adjustment, the internal pressure relaxation was carried out for 100 ps to equilibrate the system by using the NVT ($N = 1800$, $V = 23.59 \text{ \AA} \times 25.04 \text{ \AA} \times 24.16 \text{ \AA}$, $T = 298 \text{ K}$) ensemble.

Molecular dynamics simulations combined with the Monte Carlo method were performed for 100 ps by using the NVT ($N = 1800$, $V = 23.59 \text{ \AA} \times 25.04 \text{ \AA} \times 24.16 \text{ \AA}$, $T = 3000 \text{ K}$) ensemble after internal pressure relaxation. During the molecular dynamics simulations, atom motions were updated every 50 steps with a time interval of 0.1 fs, which indicated that the trajectory of the simulation was output every 0.005 ps. In that case, each molecular dynamics simulation output 20000 frames. The temperature control was based on the Berendsen thermostat algorithm with 0.1 fs damping constant in all simulations. In addition, the Monte Carlo method was applied in this system to increase the randomness of reaction to make the simulation closer to the actual reac-

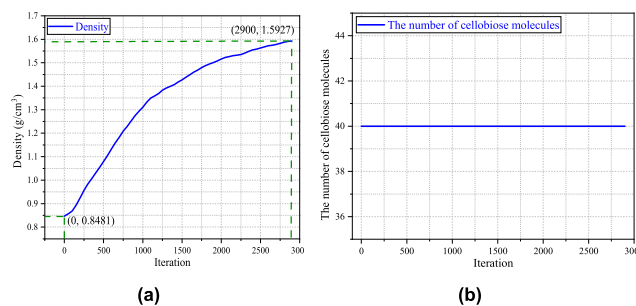


FIGURE 2. Changes in (a) the density of the system and (b) the number of cellobiose molecules in each reaction iteration steps.

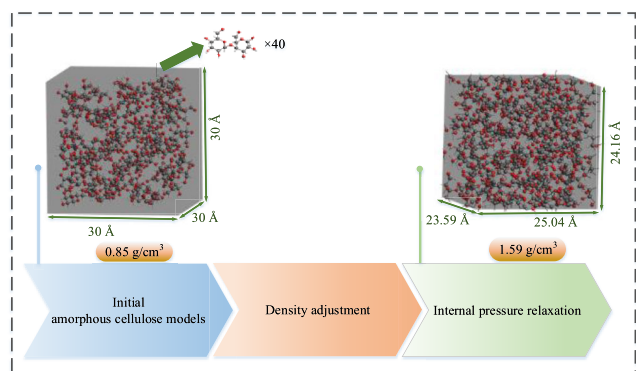


FIGURE 3. Flow diagram of the simulation.

tion conditions of transformers [34], [35]. The Monte Carlo method resolves conventional mathematical statics problems by establishing a probabilistic model to describe the reaction process [34]–[36].

The simulation flow diagram is shown in Fig. 3.

The assumptions and conditions of the cellulose model have been verified and used in many studies. Shi *et al.* [37] investigated the formation mechanism of water molecules during the pyrolysis of cellulose insulation by using the aging model of cellulose. Based on the TAD theory, the temperature of 1600 K, 1800 K, and 2000 K was set to investigate the formation mechanisms. Besides, Zhang *et al.* used the same assumptions and conditions for the cellulose model to study the reaction mechanism of methanol [38] and ethanol [31].

IV. RESULTS AND ANALYSIS

The main formation pathways of methanol are summarized through observing the formation and fracture of bonds. In all simulation figures, the atoms that are going to constitute methanol are displayed in the ball-and-stick mode and the rest are displayed in the stick mode. The formation pathways of methanol are summarized as the following three categories.

Formation pathway 1: The methylol group ($-\text{CH}_2\text{OH}$) on the 5-carbon atom of the 1-pyran ring or 4-pyran ring is detached, absorbing a hydrogen atom to form a methanol molecule. Take the reaction process of the 4-pyran ring as an example, the process of methanol formation from methylol abscission of the 4-pyran ring is shown in Fig. 4. The position of each atom that is going to generate methanol molecule is

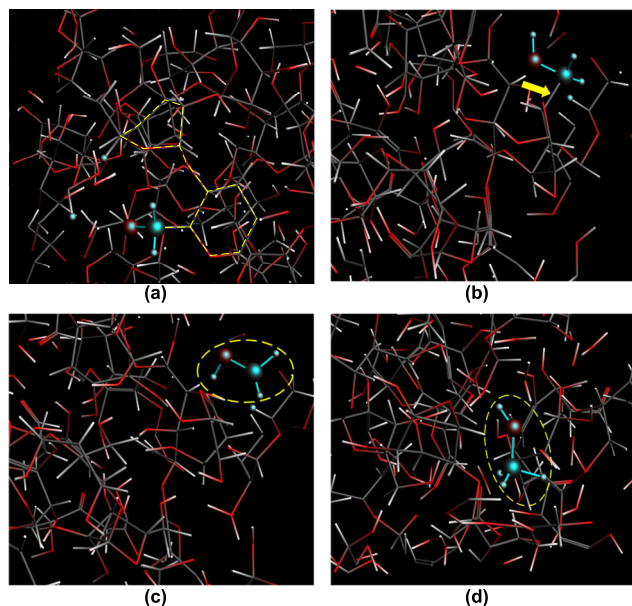


FIGURE 4. The formation of methanol from the methylol group on the 5-carbon atom of the 4-pyran ring. (a) 0.00 ps; (b) 5.35 ps; (c) 5.40 ps; (d) 5.70 ps.

highlighted. At 0 ps shown in Fig. 4a, the backbone of the cellobiose in which the methylol group ($-\text{CH}_2\text{OH}$) resides is marked by yellow dotted lines. At 5.35 ps, the C-C bond between the 5-carbon atom and 6-carbon atom of the 4-pyran ring indicated by the arrow in Fig. 4b is extremely unstable under high temperature and is going to break. After a short while, the C-C bond breaks at 5.40 ps to form a free methylol group ($-\text{CH}_2\text{OH}$), as shown in Fig. 4c. After a hydrogen atom is captured by the free methylol group ($-\text{CH}_2\text{OH}$) at 5.70 ps, a methanol molecule is formed, as shown in Fig. 4d. Zhang *et al.* [38] suggested that the methylol group ($-\text{CH}_2\text{OH}$) on the 5-carbon atom of the 1-pyran ring or 4-pyran ring is easily broken to form formaldehyde (CH_2O) due to the weak bond energy, then methanol will be generated by formaldehyde (CH_2O). In comparison, methanol is formed through the direct combination of the free methylol group ($-\text{CH}_2\text{OH}$) and the hydrogen ion in this study, without the formation of CH_2O .

Formation pathway 2: a methyl group ($-\text{CH}_3$) reacts with a highly active hydroxyl group ($-\text{OH}$) to form a methanol molecule. Most of the methyl groups ($-\text{CH}_3$) in the reaction system are attached to the molecular fragments generated by the aging of the cellulose. Two molecular fragments, in which the methyl group ($-\text{CH}_3$) and the hydroxyl group ($-\text{OH}$) are located, are marked with yellow dotted lines, as shown in Fig. 5a. The C-C bond between the methyl group ($-\text{CH}_3$) and its corresponding molecular fragment is cleaved at 70.26 ps to form a free methyl group ($-\text{CH}_3$), while the hydroxyl group ($-\text{OH}$) is still attached to the molecular fragment, as shown in Fig. 5b. Literature [16] proposed that the C-C bond between a methyl group ($-\text{CH}_3$) and the molecular fragment will break to form a free methyl group ($-\text{CH}_3$) at the high temperature. According to our simulation results, the free methyl group

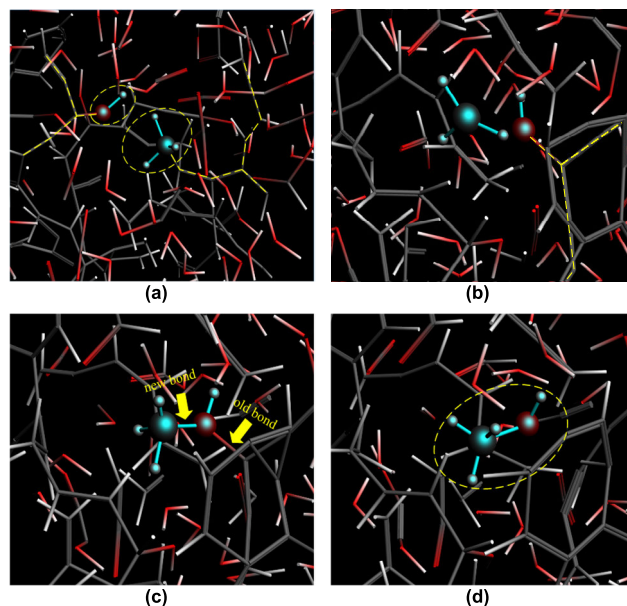


FIGURE 5. The formation of methanol from the methyl group and hydroxyl group. (a) 70.18 ps; (b) 70.26 ps; (c) 70.28 ps; (d) 70.29 ps.

($-\text{CH}_3$) is accelerated by high temperature and gradually moves closer to the hydroxyl group ($-\text{OH}$) with high activity on another molecular fragment. The bond (“old bond” in Fig. 5c) between the hydroxyl group ($-\text{OH}$) and the carbon atom of the molecular fragment is going to break while a new bond (“new bond” in Fig. 5c) is formed between the hydroxyl group ($-\text{OH}$) and the methyl group ($-\text{CH}_3$) at 70.28 ps. Then a methanol molecule is generated at 70.29 ps, as shown in Fig. 5d.

Formation pathway 3: Formaldehyde (CH_2O), which is a by-product of cellulose insulation aging, generates methanol under intense molecular thermodynamic motion. The formation pathways of formaldehyde (CH_2O) by cellulose degradation have been analyzed by Zhang *et al.* [39], [40]. Anhydroglucoses are generated during cellulose homolysis cleavage. Subsequently, these anhydroglucose molecular fragments degrade again and generate the formaldehyde molecule (CH_2O). The detailed formation pathway of the formaldehyde molecule (CH_2O) is shown in Fig. 6.

In the established simulation system, the formaldehyde molecule (CH_2O) generated by the reaction system at 78.00 ps is presented in Fig. 7a. The carbon-oxygen double bond ($\text{C}=\text{O}$) of formaldehyde (CH_2O) breaks and becomes a carbon-oxygen single bond after combining with a hydrogen atom. After that, a methylol group ($-\text{CH}_2\text{OH}$) is generated, as shown in Fig. 7b. Then, the methylol group ($-\text{CH}_2\text{OH}$) starts to attack a hydrogen atom of one fragment under the intense molecular thermal motion at 78.37 ps, as shown in Fig. 7c. After a short period of competition, the methylol group ($-\text{CH}_2\text{OH}$) captures a hydrogen atom and a methanol molecule is finally generated at 78.39 ps, as shown in Fig. 7d.

The above three formation pathways are summarized in Fig. 8. All of the formation pathways are illustrated by single

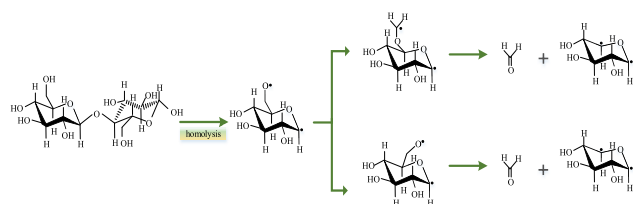


FIGURE 6. Main pathways of the formaldehyde formation during cellulose degradation.

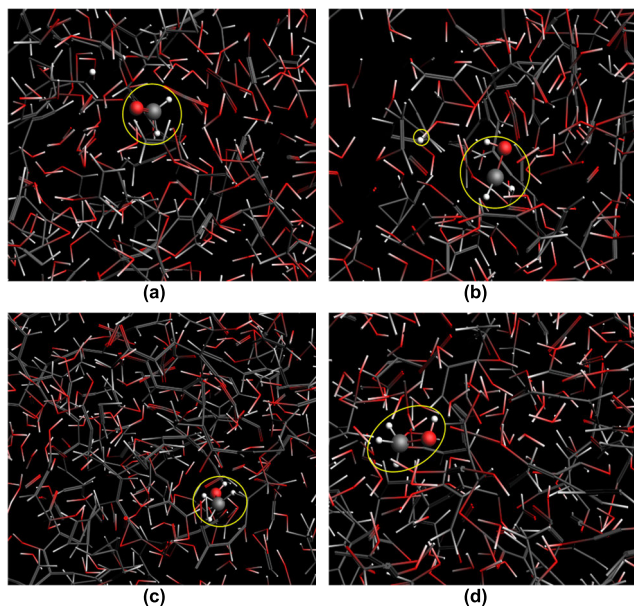


FIGURE 7. The formation of methanol from formaldehyde. (a) 78.00 ps; (b) 78.14 ps; (c) 78.37 ps; (d) 78.39 ps.

cellulose in the ball-and-stick model. The yellow wavy line indicates the bond tending to be broken, and the yellow arrow indicates the bond tending to be formed.

V. SOURCE ANALYSIS OF CARBON AND OXYGEN ATOMS OF METHANOL

To further investigate the reaction mechanisms of methanol formation during cellulose insulation aging, the main source of carbon and oxygen atoms constituting methanol molecules is fully analyzed. For brevity, each atom in this section is named by the AMS software, as shown in Fig. 9.

According to simulation results in this study, it was found that the carbon and oxygen atoms of methanol mainly come from some specific atoms on the cellobiose. The main sources of the carbon and oxygen atoms that constitute the methanol molecule are shown in Table 1, in which the source atoms less than 10% are not presented.

As can be seen from Table 1, the carbon atoms in the generated methanol molecules mainly come from C (14) and C (19) through formation pathway 1 and pathway 2. C (14) and C (19) correspond to the No. 6 carbon atom of the 1-pyran ring and 4-pyran ring respectively. These particular carbon atoms are more likely to form free groups of a single carbon atom, which greatly contributes to the formation of methanol molecules.

TABLE 1. Sources of carbon atoms and oxygen atoms of methanol molecules.

Atom	Number	Percentage (%)
C (14)	14	28.57
C (19)	14	28.57
O (20)	12	24.49
O (15)	9	18.37
O (7)	7	14.29
O (23)	5	10.2

The oxygen atoms in the generated methanol molecules mainly come from O (15) and O (20) which are connected to C (14) and C (19) respectively. O (7) and O (23) as the other two sources of oxygen atoms of methanol can be explained through the Mayer bond order proposed by Mayer in 1986 [41]. The Mayer bond order is a natural extension of the Wiberg bond order, which has been proved effective in bonding analysis using semi-empirical computational methods and the Mulliken population analysis to ab initio theories [42]. The value of the Mayer bond order reflects the relative strength of bonds in a molecular structure.

In this paper, the Mayer bond orders of cellobiose under different degradation condition were calculated using AMS software (Fig. 10 and Fig. 11). Each model of cellobiose molecules had been optimized before calculation. Fig. 10 shows the initial Mayer bond order value of cellobiose. Smaller Mayer bond order value (0.7624) of the bond between C (13) and O (23) makes it easier to break and react with a methyl group ($-\text{CH}_3$) to form a methanol molecule. It is reflected in Table 1 that O (23) is more likely to be the source of the methanol molecule rather than O (18).

The number of ruptured 1,4- β -glycosidic bonds of cellobiose increases rapidly over the aging time. Fig. 11 shows the Mayer bond order value after the cleavage of the 1,4- β -glycosidic bond of cellobiose. The Mayer bond order between C (8) and hydroxyl ($-\text{OH}$) is much smaller than that between C (8) and the surrounding atoms on the 4-pyran ring. Therefore, the hydroxyl group ($-\text{OH}$) of C (8) on the 4-pyran ring tends to fall off and reacts with other free radicals (e.g., methyl group).

VI. EFFECT OF DIFFERENT REACTION CONDITIONS ON THE FORMATION OF METHANOL

The effects of different initial conditions (moisture and oxygen) on the amount of generated methanol are studied in this paper. Four initial models are designed as follows:

a) Model 1 contains only 40 cellobiose molecules; b) Model 2 contains 40 cellobiose molecules and 15 water molecules; c) Model 3 contains 40 cellobiose molecules and 15 oxygen molecules; d) Model 4 contains 40 cellobiose molecules, 15 water molecules, and 15 oxygen molecules. Other settings are similar to the previous simulations in this work. The NPT ($P = 1000$ Mpa, $T = 50$ K) ensemble was used to perform density adjustment. After density adjustment, the internal pressure relaxation was carried out

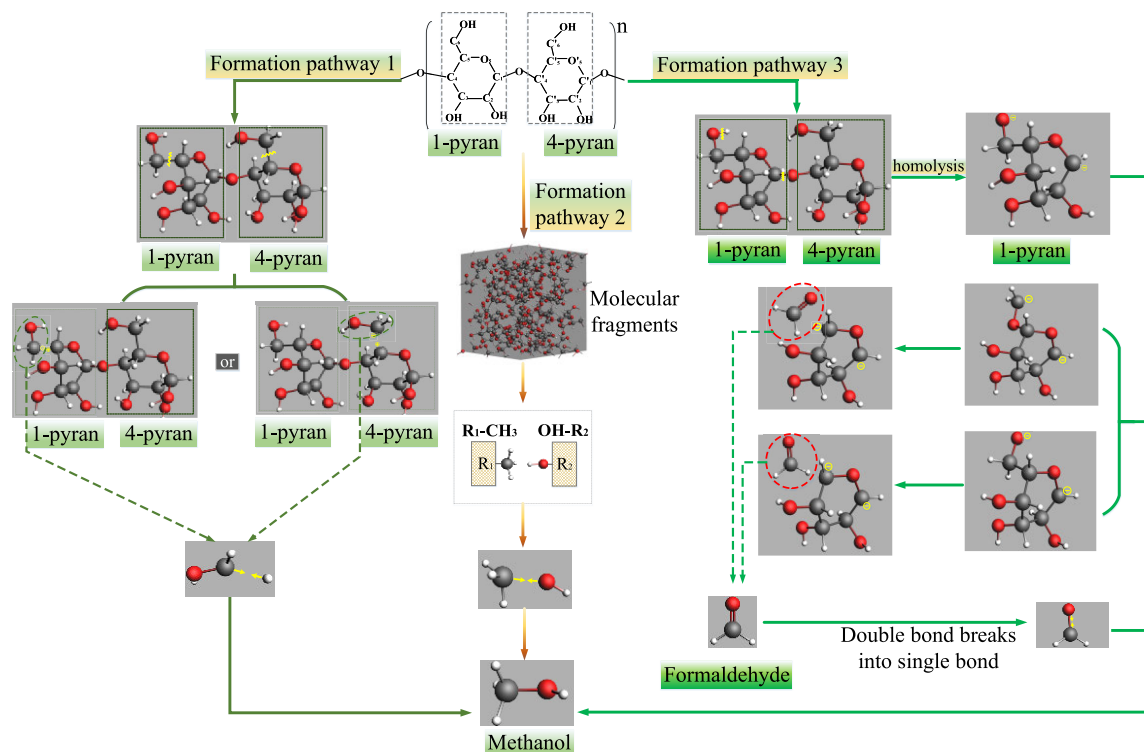


FIGURE 8. Total schematic diagram of three formation pathways of methanol. (The R_1 and R_2 represent the two molecular fragments in which the methyl group and the hydroxyl group are located respectively.)

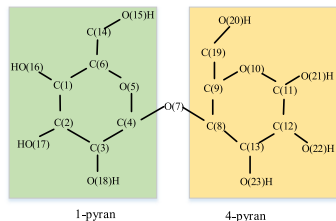


FIGURE 9. The naming of cellobiose by AMS software.

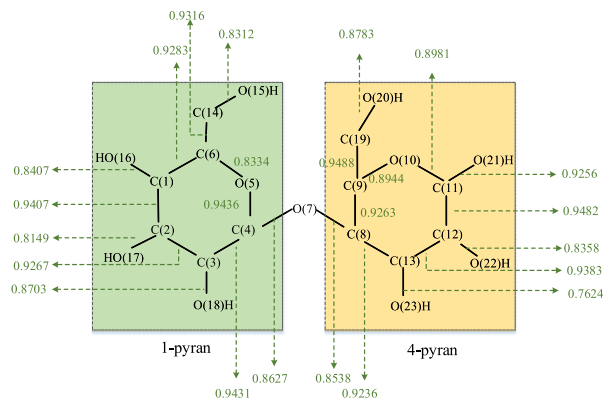


FIGURE 10. The initial Mayer bond order of cellobiose.

for 100 ps to equilibrate the system by using the NVT ensemble ($T = 298$ K). Then, molecular dynamics simulations combined with the Monte Carlo method were performed for 100 ps by using the NVT ensemble. During the molecular dynamics simulations, atom motions were updated every 50 steps with a time interval of 0.1 fs, which indicated that the trajectory of the simulation was output every 0.005 ps. The temperature control was based on the Berendsen thermostat algorithm with 0.1 fs damping constant in all simulations. The results are shown in Fig. 12.

Fig. 12a shows changes in the number of methanol molecule over time without initial moisture and oxygen. The unstable methanol molecules existing temporarily are ignored. The maximum number of methanol molecules generated without initial moisture and oxygen is 2. Fig. 12b and Fig. 12c show changes in the number of methanol molecules obtained with the addition of 15 water molecules (2% of weight) and 15 oxygen molecules (3% of weight) in the initial

model, respectively. The maximum number of methanol molecules present in Model 2 and Model 3 is only one, which indicates that the separate presence of initial moisture and oxygen inhibits the formation of methanol to a certain extent. The simulation results are consistent with several significant experiments. Aging tests were carried out by Jalbert *et al.* [9] to verify the independence of methanol on moisture. Cellulose insulation samples with 0.5%, 1%, or 2% (w/w) initial moisture content were used for aging tests. The experimental results indicated that the presence of initial moisture has no effect on methanol formation. In addition, Li *et al.* [43] proposed that when the moisture content is small, oxygen molecules will form hydrogen bonds with water molecules to prevent water from reacting with cellulose.

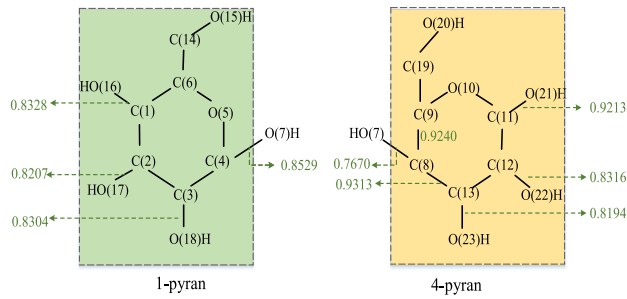


FIGURE 11. The Mayer bond order after the cleavage of the 1,4-β-glycosidic bond of cellobiose.

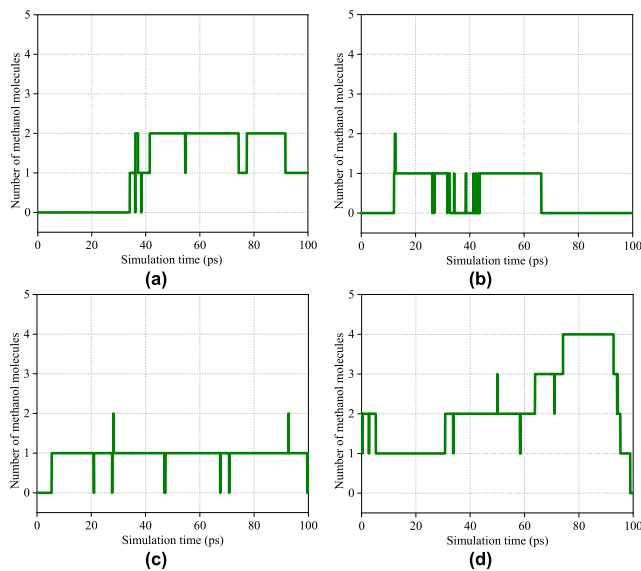


FIGURE 12. Methanol formation under different initial conditions. (a) Model 1; (b) Model 2; (c) Model 3; (d) Model 4.

In Fig. 12d, the maximum number of methanol molecules increases to 4, with the co-existence of initial moisture and oxygen in Model 4. The catalytic mechanism of moisture and oxygen on methanol formation is analyzed in this paper. Hydrocarbons in cellulose insulation react with oxygen molecules to form carboxylic acids. One water molecule deprives a hydrogen ion on the carboxylic acid, and a hydronium is formed (Fig. 13). Then, the hydrogen ion is transferred to the cellulose chain and causes chain scission (Fig. 14).

As mentioned before, the cleavage of 1,4-β-glycosidic bond contributes to the formation of methanol. According to the Brønsted-Lowry theory, carboxylic acids can react with cellulose by directly transferring hydrogen ions to it. However, water is more polar than cellulose, which makes the dehydrogenation reaction of carboxylic acids easier to occur. The results indicated that the co-existence of a large amount of oxygen and water facilitates the formation of methanol by catalyzing the acid hydrolysis of cellulose. The simulation results of the catalytic mechanism are consistent with several significant experimental studies [44]–[46].

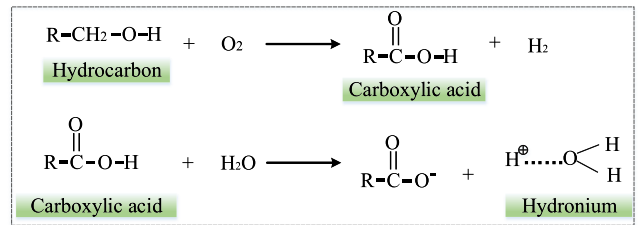


FIGURE 13. The catalytic mechanism of moisture and oxygen on methanol formation.

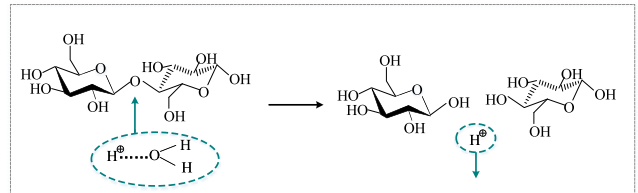


FIGURE 14. The cleavage of cellulose by hydronium.

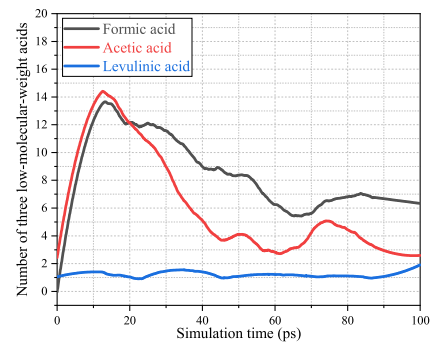


FIGURE 15. Changes in the number of three low-molecular-weight acids in cellulose with time.

It has been reported that the main degradation mechanism of cellulose is acid hydrolysis, especially for the amorphous region [15], [44], [47], [48]. With the aging of cellulose insulation, a large amount of low-molecular-weight acids (e.g. formic acid, acetic acid, and levulinic acid) will exist in cellulose insulation. Part of the low-molecular-weight acids partly comes from cellulose degradation, while others come from the oxidation of insulating oil [44], [47]. To verify the above analysis, the number of three low-molecular-weight acids were calculated based on Model 4, and the results were shown in Fig. 15. The results showed that the amount of three low-molecular-weight acids increases rapidly at the beginning of molecular dynamics simulation and decreases at 13 ps. The reason is that the combined influence of initial moisture and oxygen have accelerated the formation of three low-molecular-weight acids. However, the acid hydrolysis of cellulose insulation consumes carboxylic acids, which reduces the number of carboxylic acids. The phenomenon is consistent with the proposed catalytic mechanism and verifies the validity of the mechanism.

VII. CONCLUSION

In this paper, the formation mechanisms of methanol during the degradation of cellulose insulation were investigated by

molecular dynamics simulation using ReaxFF combined with Monte Carlo. It is of great interest to find formation mechanisms of methanol at the atomic or molecular level. The obtained results can be concluded as follows.

- I. Related simulation models were built to investigate the formation of methanol, and the results showed that there are three formation pathways of methanol during the degradation of cellulose insulation.
- II. The source of carbon atoms and oxygen atoms constituting methanol molecules was analyzed. The results confirmed that the carbon atoms mainly come from C (14) and C (19), while the oxygen atoms mainly come from O (15), O (20), O (7), and O (23).
- III. Analysis of the number of methanol molecules under different initial conditions indicated that the co-existence of initial moisture and oxygen facilitates the conversion of cellulose degradation products to methanol. In addition, the catalytic mechanism of the methanol formation under the coexistence of initial moisture and oxygen was analyzed, and the regularity of the three low-molecular-weight acids verified the validity of the mechanism.

The investigation of methanol formation through molecular dynamics simulation gives a new perspective to understand the formation mechanisms of methanol during cellulose insulation aging and provides a theoretical contribution to further studies on the evaluation of aging condition of the cellulose insulation.

REFERENCES

- [1] J. Liu, X. Fan, Y. Zhang, C. Zhang, and Z. Wang, "Aging evaluation and moisture prediction of oil-immersed cellulose insulation in field transformer using frequency domain spectroscopy and aging kinetics model," *Cellulose*, vol. 27, no. 12, pp. 7175–7189, Aug. 2020.
- [2] J. Hao, C. Liu, Y. Li, R. Liao, Q. Liao, and C. Tang, "Preparation nanostructure polytetrafluoroethylene (PTFE) functional film on the cellulose insulation polymer and its effect on the breakdown voltage and hydrophobicity properties," *Materials*, vol. 11, no. 5, p. 851, May 2018.
- [3] J. Liu, X. Fan, Y. Zhang, H. Zheng, and J. Jiao, "Temperature correction to dielectric modulus and activation energy prediction of oil-immersed cellulose insulation," *IEEE Trans. Dielectrics Electr. Insul.*, vol. 27, no. 3, pp. 956–963, Jun. 2020.
- [4] D. Feng, J. Hao, R. Liao, X. Chen, L. Cheng, and M. Liu, "Comparative study on the thermal-aging characteristics of cellulose insulation polymer immersed in new three-element mixed oil and mineral oil," *Polymers*, vol. 11, no. 8, p. 1292, Aug. 2019.
- [5] J. Liu, S. Yang, Y. Zhang, H. Zheng, Z. Shi, and C. Zhang, "A modified X-model of the oil-impregnated bushing including non-uniform thermal aging of cellulose insulation," *Cellulose*, vol. 27, no. 8, pp. 4525–4538, May 2020.
- [6] J. Liu, X. Fan, Y. Zhang, H. Zheng, and C. Zhang, "Condition prediction for oil-immersed cellulose insulation in field transformer using fitting fingerprint database," *IEEE Trans. Dielectrics Electr. Insul.*, vol. 27, no. 1, pp. 279–287, Feb. 2020.
- [7] J. Liu, X. Fan, Y. Zhang, H. Zheng, and M. Zhu, "Quantitative evaluation for moisture content of cellulose insulation material in paper/oil system based on frequency dielectric modulus technique," *Cellulose*, vol. 27, no. 4, pp. 2343–2356, Mar. 2020.
- [8] J. Liu, X. Fan, Y. Zhang, C. Zhang, and Z. Wang, "Frequency domain spectroscopy prediction of transformer oil-immersed cellulose insulation under diverse temperature and moisture," *IEEE Trans. Dielectrics Electr. Insul.*, to be published, doi: 10.1109/TDEI.2020.008813.
- [9] J. Jalbert, R. Gilbert, P. Tétreault, B. Morin, and D. Lessard-Déziel, "Identification of a chemical indicator of the rupture of 1, 4- β -glycosidic bonds of cellulose in an oil-impregnated insulating paper system," *Cellulose*, vol. 14, no. 4, pp. 295–309, 2007.
- [10] A. Schaut, S. Autru, and S. Eeckhoudt, "Applicability of methanol as new marker for paper degradation in power transformers," *IEEE Trans. Dielectrics Electr. Insul.*, vol. 18, no. 2, pp. 533–540, Apr. 2011.
- [11] R. Gilbert, J. Jalbert, S. Duchesne, P. Tétreault, B. Morin, and Y. Denos, "Kinetics of the production of chain-end groups and methanol from the depolymerization of cellulose during the ageing of paper/oil systems. Part 2: Thermally-upgraded insulating papers," *Cellulose*, vol. 17, no. 2, pp. 253–269, Apr. 2010.
- [12] J. Jalbert, R. Gilbert, Y. Denos, and P. Gervais, "Chemical markers for the determination of power transformer insulating life, a step forward," in *Proc. 76th Annu. Int. Doble Client Conf.*, 2009.
- [13] J. Jalbert, R. Gilbert, Y. Denos, and P. Gervais, "Methanol: A novel approach to power transformer asset management," *IEEE Trans. Power Del.*, vol. 27, no. 2, pp. 514–520, Apr. 2012.
- [14] R. Gilbert, J. Jalbert, P. Tétreault, B. Morin, and Y. Denos, "Kinetics of the production of chain-end groups and methanol from the depolymerization of cellulose during the ageing of paper/oil systems. Part 1: Standard wood kraft insulation," *Cellulose*, vol. 16, no. 2, pp. 327–338, Apr. 2009.
- [15] J. Jalbert, E. Rodriguez-Celis, S. Duchesne, B. Morin, M. Ryadi, and R. Gilbert, "Kinetics of the production of chain-end groups and methanol from the depolymerization of cellulose during the ageing of paper/oil systems. Part 3: Extension of the study under temperature conditions over 120°C," *Cellulose*, vol. 22, no. 1, pp. 829–848, Feb. 2015.
- [16] T. Zhao, T. Li, Z. Xin, L. Zou, and L. Zhang, "A ReaxFF-based molecular dynamics simulation of the pyrolysis mechanism for polycarbonate," *Energy Fuels*, vol. 32, no. 2, pp. 2156–2162, Feb. 2018.
- [17] C. Di Blasi, G. Signorelli, C. Di Russo, and G. Rea, "Product distribution from pyrolysis of wood and agricultural residues," *Ind. Eng. Chem. Res.*, vol. 38, no. 6, pp. 2216–2224, Jun. 1999.
- [18] M. Karplus and J. A. McCammon, "Molecular dynamics simulations of biomolecules," *Nature Structural Biol.*, vol. 9, no. 9, pp. 646–652, Sep. 2002.
- [19] A. Hospital, J. R. Goñi, M. Orozco, and J. L. Gelpi, "Molecular dynamics simulations: Advances and applications," *Adv. Appl. Bioinf. Chem., AACB*, vol. 8, no. 37, pp. 37–47, 2015.
- [20] K. Mazeau and L. Heux, "Molecular dynamics simulations of bulk native crystalline and amorphous structures of cellulose," *J. Phys. Chem. B*, vol. 107, no. 10, pp. 2394–2403, Mar. 2003.
- [21] H. Liu, K. L. Sale, B. M. Holmes, B. A. Simmons, and S. Singh, "Understanding the interactions of cellulose with ionic liquids: A molecular dynamics study," *J. Phys. Chem. B*, vol. 114, no. 12, pp. 4293–4301, Apr. 2010.
- [22] J. M. Haile, I. Johnston, A. J. Mallinckrodt, and S. McKay, "Molecular dynamics simulation: Elementary methods," *Comput. Phys.*, vol. 7, no. 6, p. 625, 1993.
- [23] R. Du, A. Zhang, Z. Du, and X. Zhang, "Molecular dynamics simulation on thin-film lubrication of a mixture of three alkanes," *Materials*, vol. 13, no. 17, p. 3689, Aug. 2020.
- [24] M. F. Russo and A. C. T. van Duin, "Atomistic-scale simulations of chemical reactions: Bridging from quantum chemistry to engineering," *Nucl. Instrum. Methods Phys. Res. B: Beam Interact. Mater. At.*, vol. 269, no. 14, pp. 1549–1554, Jul. 2011.
- [25] A. C. T. van Duin, S. Dasgupta, F. Lorant, and W. A. Goddard, III, "ReaxFF: A reactive force field for hydrocarbons," *J. Phys. Chem. A*, vol. 105, no. 41, pp. 9396–9409, 2001.
- [26] K. Chenoweth, A. C. T. van Duin, I. William, and A. Goddard, "ReaxFF reactive force field for molecular dynamics simulations of hydrocarbon oxidation," *J. Phys. Chem. A*, vol. 112, no. 5, pp. 1040–1053, 2008.
- [27] C. Ashraf, S. Shabnam, A. Jain, Y. Xuan, and A. C. T. van Duin, "Pyrolysis of binary fuel mixtures at supercritical conditions: A ReaxFF molecular dynamics study," *Fuel*, vol. 235, pp. 194–207, Jan. 2019.
- [28] A. C. T. van Duin and J. S. S. Damsté, "Computational chemical investigation into isorenieratene cyclisation," *Organic Geochem.*, vol. 34, no. 4, pp. 515–526, Apr. 2003.
- [29] B. D. Jensen, A. Bandyopadhyay, K. E. Wise, and G. M. Odegard, "Parametric study of ReaxFF simulation parameters for molecular dynamics modeling of reactive carbon gases," *J. Chem. Theory Comput.*, vol. 8, no. 9, pp. 3003–3008, Sep. 2012.

- [30] O. H. Arroyo, I. Fofana, J. Jalbert, and M. Ryadi, "Relationships between methanol marker and mechanical performance of electrical insulation papers for power transformers under accelerated thermal aging," *IEEE Trans. Dielectrics Electr. Insul.*, vol. 22, no. 6, pp. 3625–3632, Dec. 2015.
- [31] Y. Zhang, Y. Li, S. Li, H. Zheng, and J. Liu, "A molecular dynamics study of the generation of ethanol for insulating paper pyrolysis," *Energies*, vol. 13, no. 1, p. 265, Jan. 2020.
- [32] M. R. Soerensen and A. F. Voter, "Temperature-accelerated dynamics for simulation of infrequent events," *J. Chem. Phys.*, vol. 112, no. 21, pp. 9599–9606, Jun. 2000.
- [33] J. Brandrup, E. H. Immergut, E. A. Grulke, A. Abe, and D. R. Bloch, Eds., *Polymer Handbook*, vol. 89. New York, NY, USA: Wiley, 1999.
- [34] K. Binder, Ed., *Monte Carlo and Molecular Dynamics Simulations in Polymer Science*. New York, NY, USA: Oxford Univ. Press, 1995.
- [35] K. Binder, "Applications of Monte Carlo methods to statistical physics," *Rep. Prog. Phys.*, vol. 60, no. 5, p. 487, 1997.
- [36] X. Xiao, W. Yang, L. Li, T. Zhong, and X. Zhang, "Application of molecular simulation in transformer oil–paper insulation," *J. Eng.*, vol. 2019, no. 16, pp. 1324–1327, Mar. 2019.
- [37] L. Shi, T. Zhao, G. Shen, Y. Hou, L. Zou, and L. Zhang, "Molecular dynamics simulation on generation mechanism of water molecules during pyrolysis of insulating paper," in *Proc. IEEE Int. Conf. High Voltage Eng. Appl. (ICHVE)*, Sep. 2016, pp. 1–4.
- [38] Y. Zhang, Y. Li, H. Zheng, M. Zhu, J. Liu, T. Yang, C. Zhang, and Y. Li, "Microscopic reaction mechanism of the production of methanol during the thermal aging of cellulosic insulating paper," *Cellulose*, vol. 27, no. 5, pp. 2455–2467, Mar. 2020.
- [39] X. Zhang, J. Li, W. Yang, and W. Blasiak, "Formation mechanism of levoglucosan and formaldehyde during cellulose pyrolysis," *Energy Fuels*, vol. 25, no. 8, pp. 3739–3746, Aug. 2011.
- [40] X. Zhang, W. Yang, and W. Blasiak, "Kinetics of levoglucosan and formaldehyde formation during cellulose pyrolysis process," *Fuel*, vol. 96, pp. 383–391, Jun. 2012.
- [41] I. Mayer, "Bond orders and valences from ab initio wave functions," *Int. J. Quantum Chem.*, vol. 29, no. 3, pp. 477–483, Mar. 1986.
- [42] A. J. Bridgeman, G. Cavigliasso, L. R. Ireland, and J. Rothery, "The Mayer bond order as a tool in inorganic chemistry," *J. Chem. Soc., Dalton Trans.*, vol. 14, pp. 2095–2108, Mar. 2001.
- [43] Y. Li, G. Wu, W. Li, Y. Cui, and B. Gao, "Influence of moisture and oxygen on aging of oil-paper insulation," in *Proc. Annu. Rep. Conf. Electr. Insul. Dielectric Phenomena*, Oct. 2013, pp. 120–123.
- [44] L. E. Lundgaard, W. Hansen, S. Ingebrigtsen, D. Linhjell, and M. Dahlund, "Aging of kraft paper by acid catalyzed hydrolysis," in *Proc. IEEE Int. Conf. Dielectric Liquids, (ICDL)*, Jun./Jul. 2005, pp. 381–384.
- [45] Q. Xiang, Y. Y. Lee, P. O. Pettersson, and R. W. Torget, "Heterogeneous aspects of acid hydrolysis of α -cellulose," in *Biotechnology for Fuels and Chemicals*. Totowa, NJ, USA: Humana Press, 2003, pp. 505–514.
- [46] L. E. Lundgaard, W. Hansen, D. Linhjell, and T. J. Painter, "Aging of oil-impregnated paper in power transformers," *IEEE Trans. Power Del.*, vol. 19, no. 1, pp. 230–239, Jan. 2004.
- [47] N. Lelekakis, J. Wijaya, D. Martin, and D. Susa, "The effect of acid accumulation in power-transformer oil on the aging rate of paper insulation," *IEEE Elect. Insul. Mag.*, vol. 30, no. 3, pp. 19–26, May 2014.
- [48] J. Jalbert, E. M. Rodriguez-Celis, and O. H. Arroyo-Fernández, "Methanol marker for the detection of insulating paper degradation in transformer insulating oil," *Energies*, vol. 12, no. 20, p. 3969, Oct. 2019.



JIEFENG LIU (Member, IEEE) was born in Hebei, China, in 1985. He received the M.Sc. and Ph.D. degrees in electrical engineering from Chongqing University, Chongqing, China, in 2011 and 2015, respectively. From 2015 to 2018, he worked with State Grid Shijiazhuang Electric Power Supply Company, where he is currently an Engineer of electrical engineering. In 2018, he joined Guangxi University, where he is also an Assistant Professor. He is the author and coauthor of more than 40 articles published in journals and conferences. His research interests include condition assessment and intelligent diagnosis on high voltage electrical apparatus.



HUAN ZHAO was born in Guizhou, China, in 1993. She received the bachelor's degree in electrical engineering from the Taiyuan University of Technology, in 2017. She is currently pursuing the master's degree in electrical engineering with Guangxi University, Nanning, China. Her current research interests include condition assessment and fault diagnosis of high-voltage electrical equipment.



XIANHAO FAN (Student Member, IEEE) was born in Gansu, China, in 1995. He received the bachelor's degree in electrical engineering from Guangxi University, Nanning, China, in 2018, where he is currently pursuing the Ph.D. degree. He is the author and coauthor of over ten articles published in SCI journals. His current research interests include insulation condition assessment and insulation fault diagnosis for transformers.



YIYI ZHANG (Member, IEEE) was born in Guangxi, China, in 1986. He received the bachelor's degree in electrical engineering from Guangxi University, Nanning, China, in 2008, and the Ph.D. degree in electrical engineering from Chongqing University, Chongqing, China, in 2014. In 2014, he joined Guangxi University, where he is currently an Associate Professor with the College of Electrical Engineering. He was awarded by the Bagui Young Talent Scholar (the Young Talent in Guangxi province) and the Guangxi thousand teachers' talent (the young teacher talents in Guangxi province) in 2019 and 2017, respectively. He hosts over ten projects and is the author and coauthor of over 60 articles published in SCI/EI journals and conferences. His current research interest includes the intelligent diagnosis for transformers.

• • •